

Research Article

Open Access



# Active manipulation of a tethered drone using explainable AI

Shraddha Barawkar<sup>1</sup>, Manish Kumar<sup>1,2</sup>

<sup>1</sup>Maryland Robotics Center, University of Maryland, College Park, MD 20740, USA.

<sup>2</sup>Mechanical and Materials Engineering, University of Cincinnati, Cincinnati, OH 45221, USA.

**Correspondence to:** Dr. Shraddha Barawkar, Maryland Robotics Center, University of Maryland, 8125 Paint Branch Dr, College Park, MD 20740, USA. E-mail: sbarawka@umd.edu

**How to cite this article:** Barawkar S, Kumar M. Active manipulation of a tethered drone using explainable AI. *Complex Eng Syst* 2024;4:6. <http://dx.doi.org/10.20517/ces.2023.33>

**Received:** 29 Sep 2023 **First Decision:** 4 Jan 2024 **Revised:** 31 Jan 2024 **Accepted:** 7 Mar 2024 **Published:** 25 Mar 2024

**Academic Editor:** Hamid Reza Karimi **Copy Editor:** Fanglin Lan **Production Editor:** Fanglin Lan

## Abstract

Tethered drones are currently finding a wide range of applications such as for aerial surveillance, traffic monitoring, and setting up ad-hoc communication networks. However, many technological gaps are required to be addressed for such systems. Most commercially available tethered drones hover at a certain position; however, the control task becomes challenging when the ground robot or station needs to move. In such a scenario, the drone is required to coordinate its motion with the moving ground vehicle without which the tether can destabilize the drone. Another challenging aspect is when the system is required to operate in GPS denied environments, such as in planetary exploration. In this paper, to address these issues, we take advantage of passive or force-based control in which the tension in the tether is sensed and used to drive the drone. Fuzzy logic is used to implement the force-based controller as a tool for explainable Artificial Intelligence. The proposed fuzzy logic controller takes tether force and its rate of change as the inputs and provides desired attitudes as the outputs. Via simulations and experiments, we show that the proposed controller allows effective coordination between the drone and the moving ground rover. The rule-based feature of fuzzy logic provides linguistic explainability for its decisions. Simulation and experimental results are provided to validate the novel controller. This paper additionally develops an adaptive controller for estimating unknown constant winds on these tethered drone systems using a proportional controller. The simulation results demonstrate the effectiveness of the proposed adaptive control scheme in addressing the effect of wind on a tethered drone.

**Keywords:** Active manipulation, tethered drone, fuzzy logic, explainable AI, force control



© The Author(s) 2024. **Open Access** This article is licensed under a Creative Commons Attribution 4.0 International License (<https://creativecommons.org/licenses/by/4.0/>), which permits unrestricted use, sharing, adaptation, distribution and reproduction in any medium or format, for any purpose, even commercially, as long as you give appropriate credit to the original author(s) and the source, provide a link to the Creative Commons license, and indicate if changes were made.



## 1. INTRODUCTION

Today, artificial intelligence (AI) is seeing widespread applications in sectors such as defense, finance, law, in healthcare and in robotics. This has been facilitated by recently developed diverse tools and methods, tremendous improvement in computational resources, and ability to gather data. Random forests<sup>[1]</sup>, reinforcement learning<sup>[2,3]</sup>, recurrent neural nets<sup>[4]</sup>, probabilistic graphical models, and deep learning<sup>[5]</sup> are a few of the recent methods that have fueled the growth of the AI field. The performance and accuracy of many of these methods have an inverse relation with the explainability. The higher performance or more accurate methods, such as deep learning, are less explainable while the most explainable techniques, such as decision trees, are less accurate<sup>[6-9]</sup>. The question is how to convert the current machine learning techniques from black box to at least partial or fully explainable solutions. This step is necessary to be addressed given the advent of AI and its widespread use is expected to be seen in the future. Moreover, it is desired to have improved accuracy with increasingly explainable models. This paper proposes the use of a fuzzy logic controller for the control of an actively tethered drone. Fuzzy logic forms a qualitative approach and a unique tool of AI used to interpret and understand complex numerical data since it can efficiently deal with inaccuracies and uncertainties<sup>[10]</sup>. The fuzzy rules are typically designed using human intuitive knowledge, and the fuzzy controller provides full interpretability to the decisions it takes as compared to limited explainability/transparency of other machine learning models. Fuzzy logic also shows better sensor noise handling capacity which enables the use of low-cost noisy sensors<sup>[11-13]</sup>. Due to the above-mentioned advantages, it was chosen as the proposed method to address the complexity and uncertainties associated with force-based coordination between a moving vehicle/robot and a tethered drone. Moreover, its widespread use in the robotics field forms an added advantage and provides more reason to exploit it as an AI tool<sup>[14-16]</sup>.

Tethered drone systems form the future of the drone industry. Such systems will be seen tomorrow providing next generation ad-hoc wireless networks<sup>[17]</sup>, carrying out infrastructure inspections, for disaster mitigation<sup>[3]</sup> or to monitor ground traffic. The need of this technology is also evident from the current market of such systems. Elistair<sup>[18]</sup>, Fotokite<sup>[19]</sup>, and Hoverfly<sup>[20]</sup> are a few of the leading companies in the area of tethered drones. As compared to traditional drones, tethered drones offer various perks such as unlimited flight time (continuous power via tether), faster and secure data transmission, safer operation, better aerial surveillance, and no fear of communication loss. Active manipulation of tethered drones, where tension in tether controls the drone actuation so the drone can be maneuvered using the tether, forms the need of the hour. This is because, to the best of our knowledge, existing tethered drone solutions are not designed to move/coordinate with a moving ground station or rover which forms a technological gap this paper attempts to address. Moreover, active manipulation of drones alleviates the need of knowledge of drone piloting skills<sup>[11,21]</sup>. Such actively manipulated tethered drones can be attached to a moving emergency vehicle, robot, or even a ship. When the ground entity (car, robot, etc.) moves, the drone is required to coordinate with the motion of the ground entity. Given the benefits offered by such systems, these drones can be leashed with ground rovers in space too for interplanetary exploration where there are no obstacles such as trees, buildings and electric wires. Such systems are especially suited for space applications due to unlimited flight time and safer operation during an emergency or technical malfunction.

Active manipulation of the tethered drone can be achieved via either position control (using sensors such as GPS or cameras to estimate the relative position of the ground robot with respect to the drone) or force control (based on the tether tension). The paper focuses on a force-based control method that enables the use of such systems in GPS denied environments such as mines, space and remote construction sites. In this approach, the tethered drone is not required to know its position or the position of the ground robot. A force sensor can be attached to the drone or the ground vehicle to implement the controller. This research is inspired by force-based control or passive control used for applications such as multi-drone cooperative transport (CT) and human-drone interaction (HDI) tasks. Both these tasks have recently been investigated by multiple researchers via schemes of admittance and fuzzy controllers<sup>[22-24]</sup>. Barawkar *et al.*<sup>[11]</sup> show both these tasks using fuzzy logic

via a low-cost imprecise force-torque sensor. In all these schemes, leader-follower strategy is utilized where the leader can either be another drone (for CT) or a human operator (for HDI). The same concept can be utilized for active manipulation of tethered drones where the motion of a ground robot controls the motion of the drone via force feedback. However, now, the coupled dynamics between the ground robot and the drone changes the challenges as compared to that of multi-drone CT and HDI tasks. For example, the maintenance of a certain tension in the tether, development of controllers for force-based coordination between the ground and aerial robots and wind disturbances form a few of the challenges associated with tethered drone systems.

In the context of force-based control of tethered drones, relatively little has been carried out in literature. Breese *et al.* [25] present a fuzzy logic force-based control of a tethered drone; however, the inputs to the fuzzy controller are different from the ones of the proposed controller of this paper. Moreover, the approach and the utilized principle are different and experiments have not been conducted. The minimization principle of forces and their rates (indicated in the Approach Section) has not been used by Breese *et al.* [25]. Wind disturbance handling is also not examined by them [25].

Drone-ground rover cooperation has been a topic of immense interest recently among the robotics research community [26,27]. However, the system dynamics and, hence, modeling and control significantly change upon introducing a tether as a means of connecting the ground robot and the drone. Further, diverse research has been conducted on tethered drone systems with different control approaches, configurations and applications. Research by Fagiano *et al.* [28] shows a control approach for chain of multiple tethered drones where the first drone is tethered to the ground station while the last drone acts as an end effector. The tethers are assumed to be elastic and their length can be varied via actuated winches installed on ground stations and drones. Each drone uses a distributed linear controller, and a high-level model predictive controller is employed to control the formation. On the other hand, Martinez Rocamora Jr *et al.* [29] develop “Oxpecker”, a tethered drone for inspection of stone-mine pillars. A multi-agent Q-learning approach is examined in another research [17] for using an optimal tethered drone in A2G communication network. Work of Lee *et al.* [30] implements a geometric controller that shows asymptotic stability of the coupled dynamics of the drone and tether of a tethered drone system.

Work of Kourani *et al.* [31] presents surge velocity control of an unmanned aerial vehicle manipulating the velocity of a buoy via tether. Further, Glick *et al.* [32] present a unified model approach to control tethered drones with state and input constraints. Work of Sandino *et al.* [33] investigates tether configurations for stability during hovering of small helicopters. The taut cable is considered as a control input which makes sure the helicopter is stable in windy environments, while an actuated winch controls the tether tension as the drone controls its position. Work of Nicotra *et al.* [34] presents nonlinear control of a tethered drone specially analyzing the taut cable case. The paper shows that the tethered drone maintains a non-zero attitude hovering at a constant position. The control objective of Nicotra *et al.* [34] is to stabilize the drone and keep the tether taut at all times which forms as a constraint. Stability is ensured by a cascade controller scheme using thrust vectoring while a reference governor ensures constraint satisfaction. Their work [34] uses a winch system to control the length of the tether, while the drone maintains its desired orientation and the tether tension. In this paper, for simplicity purposes, we do not use a winch system. The tether is assumed to be elastic and its length is fixed (not varying, as seen in winch systems). In summary, apart from our previous work [25], hardly any methods available in literature focus on developing a controller that would allow the drone to follow a ground vehicle based on tether tension inputs.

In the analysis of wind disturbances on tethered drones, very little work exists in literature. For drones in general, Mokhtari *et al.* [35] investigate the effect of wind on rotational dynamics of a drone; however, presence of tether changes the dynamics significantly. Ali *et al.* [36] discuss control of the hexrotor drone equipped with a cable-driven gripper, subject to wind disturbances, using model reference adaptive control with an integrator.

On the other hand, Escareno *et al.* [37] present trajectory control of a drone under two-dimensional wind disturbances using hierarchical, sliding mode and adaptive control techniques with an approach different from what is presented in this paper in terms of analysis of dynamics of a tethered drone. In another work, Kumar *et al.* [38] have demonstrated the performance of a tethered tilt-rotor quadcopter in rejecting wind disturbances.

In this paper, we propose a fuzzy logic-based force feedback controller for the tethered drone. We assume the contact forces and their rates between the drone and the tether are measurable. The inputs to the fuzzy logic force feedback controller are the contact forces and their rates while the output of the controller is the desired orientation required to be commanded to the attitude controller of the drone. The fuzzy rules are designed to provide effective force-based coordination between the drone and the ground robot. Both extensive simulations and experimental results are provided to validate the proposed controller. It should be noted that fuzzy logic was chosen as it enables incorporation of human intuitive knowledge (thus providing explainability) into controller design, allows for the use of noisy force sensors, and has also shown promising results previously for multi-drone CT [11].

Moreover, as external wind disturbances can mislead a force feedback controller, this paper additionally proposes an adaptive control method based on proportional force feedback for controlling an actively tethered drone in presence of constant or slowly varying unknown winds. The overall dynamic model is provided and examined thoroughly in simulations for the scenario of wind disturbance on a tethered drone. The estimation of unknown wind speed is achieved by a novel adaptive strategy that requires the drone to know the position and velocity of the ground robot. The estimated wind velocity is used by a proportional controller to control the drone.

To summarize, the primary contribution of this paper is to develop a novel and explainable force-based fuzzy logic controller for actively manipulating a tethered drone. To the best of our knowledge, this work forms one of the first instances to experimentally demonstrate force-based control of a tethered drone using low-cost imprecise force sensors. Secondly, as discussed earlier, wind disturbances can affect the force-based controller of a tethered drone. This paper additionally implements an adaptive controller on a tethered drone to estimate constant unknown wind, which forms the second primary contribution of this paper. To develop the adaptive control for the scenario of wind disturbances, we take motivation from previously utilized adaptive controllers for multi-ground robot CT where such controllers were utilized to estimate uncertainties in the object and the ground robots. However, extending previous work to a tethered drone with wind disturbances is a novel contribution due to significant difference in dynamics and control objectives. The proposed control schemes are resilient in handling wind disturbance through adaptive controllers and managing force sensor noise by employing fuzzy logic [11].

## 2. PROBLEM FORMULATION

Consider a drone tethered to a ground rover [Figure 1]. Let  $\eta_o = [\phi_o \ \theta_o \ \psi_o]^T$  be the orientation of the drone with angles roll ( $\phi_o$ ), pitch ( $\theta_o$ ), and yaw ( $\psi_o$ ). Three primary challenges are associated with operating this system. First, irrespective of stationary or moving ground rover, the drone is required to maintain a desired tension  $T^d$  in the tether and a desired tether inclination angle with the ground  $\alpha^d$ . Second, when the ground rover is moving, the drone is required to coordinate with the ground rover based on the measured tether forces and their rates ( $F^m$  and  $\dot{F}^m$ ) exerted by the ground rover on the tethered drone. This can be achieved by changing the attitude of the drone, which would allow the drone to move in order to comply with the tension in the tether. Thus, the net desired orientation  $\eta_o^d$  of the tethered drone should be a function:

$$\eta_o^d = f(T^d, \alpha^d, F^m, \dot{F}^m) \quad (1)$$

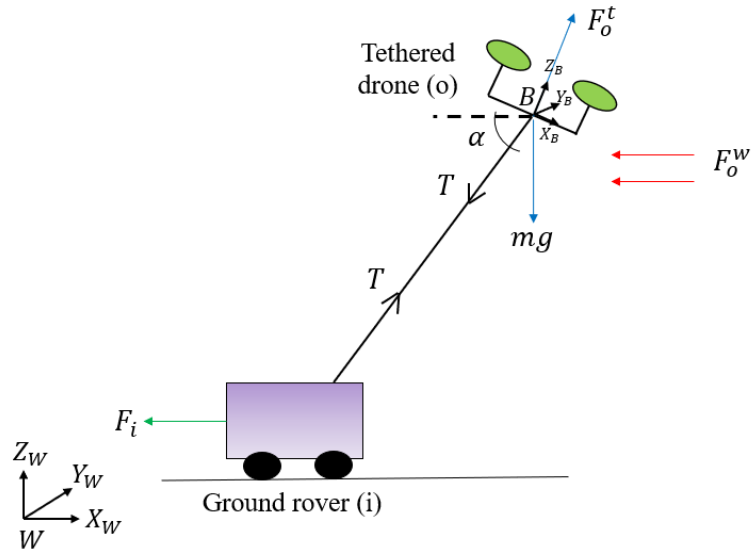


**Figure 1.** Schematic diagram of a drone tethered to a ground rover in equilibrium/hovering position.

Lastly, the next problem consists of evaluating  $f$ .

### 3. DYNAMICS

#### 3.1. General system dynamics

Figure 1 shows a schematic diagram of a drone of mass  $m$  tethered to a ground robot.  $W$  and  $B$  are the world frame of the system and the body frame of the drone, respectively. The diagram also presents different forces acting on both the drone and the ground rover at equilibrium condition in which the drone is moving at constant speed with the magnitude and the direction of motion same as that of the ground rover. The drone is assigned symbol ‘ $o$ ’ while the ground rover is assigned symbol ‘ $i$ ’. At equilibrium, the control of the drone is designed to align the pitch axis of its body frame to the direction of motion of the ground vehicle. Thus, it does not need to roll or yaw in this state (the desired roll and yaw angles,  $\phi_o^d = \psi_o^d = 0$ ). In the equilibrium condition, the drone only pitches by angle  $\theta_o^{eq}$  (equilibrium pitch angle of the drone) to create the required tension in the tether and the motion of the drone. In order to compute the desired pitch angle at equilibrium or hovering position, we perform the following analysis.

Overall, three forces act on the drone in the tethered position, viz., the tether tension ( $T$ ), the drone actuation force or thrust force due to rotors ( $F_o^t$ ), and the weight of the drone ( $mg$ ), respectively, where  $g$  is the acceleration due to gravity. It should be noted that  $F_o^w$  denotes the force due to wind disturbance which will be considered later in sections of wind disturbance analysis. Now, the force acting on the drone  $F_o^a = [F_x^a \quad F_y^a \quad F_z^a]^T$  (in world frame  $W$ ) due to actuation of the rotors is given by:

$$F_o^a = R_B^W \begin{bmatrix} 0 \\ 0 \\ F_o^t \end{bmatrix} \tag{2}$$

where  $F_o^t = (f_1 + f_2 + f_3 + f_4)$  is the thrust force (in frame  $B$ ) created by the drone which corresponds to the summation of rotor forces ( $f_1, f_2, f_3, f_4$ ), and  $R_B^W$  is the rotation matrix to go from body ( $B$ ) to world frame ( $W$ ) (see Figure 1). We use the Euler sequence of  $Z - X - Y$  to model the rotation matrix of the system in the

world frame. The rotation matrix  $R_B^W$  is:

$$R = \begin{bmatrix} c\psi c\theta - s\phi s\psi s\theta & -c\phi s\psi & c\psi s\theta + s\phi s\psi c\theta \\ c\theta s\psi + c\psi s\phi s\theta & c\phi c\psi & s\psi s\theta - c\psi c\theta s\phi \\ -c\phi s\theta & s\phi & c\phi c\theta \end{bmatrix} \quad (3)$$

where  $c(\cdot)$  and  $s(\cdot)$  are the cosine and sine terms, respectively. Upon analysis of the free body diagram, at equilibrium, we have:

$$F_x^a = T \cos(\alpha) \quad (4)$$

$$F_z^a = T \sin(\alpha) + mg \quad (5)$$

By linearizing Equation 2, we can compute the desired pitch angle ( $\theta_o^{eq}$ ) to maintain a desired tension ( $T^{eq} = [T_x^{eq} \ T_y^{eq} \ T_z^{eq}]^T$ ) in tether and desired angle ( $\alpha^{eq}$ ) of tether with the ground. Thus,  $\theta_o^{eq}$  can be computed using:

$$\theta_o^{eq} = \tan^{-1} \left( \frac{T^{eq} \cos(\alpha^{eq})}{T^{eq} \sin(\alpha^{eq}) + mg} \right) \quad (6)$$

To compute the hovering rotor speed  $\omega_o^h$  of the drone, we compute the total equilibrium force  $F_o^{eq}$  acting on the drone as follows:

$$F_o^{eq} = \sqrt{(T^{eq} \cos(\alpha^d))^2 + (T^{eq} \sin(\alpha^d) + mg)^2} \quad (7)$$

The hovering speed  $\omega_o^h$  of the drone is,

$$\omega_o^h = \sqrt{\frac{F_o^{eq}}{4k_f}} \quad (8)$$

Here,  $k_f = 2.2 \times 10^{-4}$  is the chosen motor constant ([39]). The next step consists of writing the equations of motion of the drone and the ground rover. The translational and rotational equations of motion of the tethered drone are given by,

$$m\ddot{r}_o = R_B^W \begin{bmatrix} 0 \\ 0 \\ F_o^t \end{bmatrix} + \begin{bmatrix} 0 \\ 0 \\ -mg \end{bmatrix} - T \quad (9)$$

$$I\ddot{\eta}_o = \begin{bmatrix} L(f_2 - f_4) \\ L(f_3 - f_1) \\ M_1 - M_2 + M_3 - M_4 \end{bmatrix} - \eta_o \times I\dot{\eta}_o \quad (10)$$

where  $r_o$  is the position of the drone in world frame ( $W$ ).  $I$  and  $L$  are the mass moment of inertia and the arm length of the drone, respectively.  $M_1, M_2, M_3$ , and  $M_4$  are the moments created by the four rotors of the drone.  $\eta_o = [\phi_o \ \theta_o \ \psi_o]^T$  is the orientation of the drone. It should be noted that a small angle approximation is assumed in the entire paper. Thus, angular velocity and angular acceleration of the drone are  $\dot{\eta}$  and  $\ddot{\eta}$ , respectively. We then compute the net desired pitch angle  $\theta_o^d$  and yaw angle  $\psi_o^d$  as follows:

$$\theta_o^d = \theta_o^{eq} + \theta_o^f \quad (11)$$

$$\psi_o^d = \psi_o^f \quad (12)$$

where,

$$\theta_o^f = \text{func}_1(F_x^m - T_x^{eq}, \dot{F}_x^m) \quad (13)$$

$$\psi_o^f = \text{func}_2(F_y^m, \dot{F}_y^m) \quad (14)$$

where  $F^m = [F_x^m \ F_y^m \ F_z^m]^T$  is the measured force at the point of contact between the drone and the tether. Here,  $\theta_o^f$  and  $\psi_o^f$  are the pitch and yaw commands (additional to being applied at equilibrium) to enable the

drone to follow the ground robot. It is worth noting that we calculate this sensed force mathematically for simulation analysis, while for experiments, we use a force sensor using load cells.  $func_1$  and  $func_2$  are the proposed fuzzy logic functions that evaluate the desired pitch  $\theta_o^f$  and yaw  $\psi_o^f$  angles based on the contact forces and their rates. The net desired pitch and yaw angles,  $\theta_o^d$  and  $\psi_o^d$ , are then commanded to the attitude controller of the drone thus making the drone coordinate with the ground robot based on the measured forces. The ground rover actively manipulates the drone without requiring to know the three-dimensional position of the drone. Such techniques are especially beneficial for GPS denied environments and planetary explorations. Note that we assume that the tether is elastic and there is no separately implemented controller for the vertical  $Z_W$  axis of the drone. The drone is made to operate at hovering speed  $\omega_o^h$  and the desired orientation that allows it to obtain its position along vertical  $Z_W$  direction based on the tether length.

### 3.2. System dynamics in presence of wind disturbance

This section formulates dynamics of the system considering force due to wind disturbance. Referring to Figure 1, we first write the general nonlinear form of dynamical equations of the drone as:

$$u_o - T = M_o(p_o)\ddot{p}_o + C_o(p_o, \dot{p}_o)\dot{p}_o + g_o(p_o) \quad (15)$$

where,  $p_o = \begin{bmatrix} r_o^T & \eta_o^T \end{bmatrix}^T$  is the position and orientation vector of the drone in the world fame  $W$ .  $M_o$ ,  $C_o$ ,  $g_o$ , and  $u_o$  are the symmetric positive definite inertia matrix, damping coefficient matrix, gravity force term, and the input to the drone, respectively. Note that  $\dot{M}_o - 2C_o$  is skew-symmetric for a certain  $C_o$ . Now, for a given arbitrarily defined velocity  $v_o$ , we can write

$$F_o^w = M_o(p_o)\dot{v}_o + C_o(p_o, \dot{p}_o)v_o + g_o(p_o) \quad (16)$$

where  $F_o^w$  is the force due to wind which we propose to estimate using an adaptive control strategy as presented in the next section. The input  $u_o$  provides asymptotic stability in wind disturbance and makes the drone cooperate with the ground robot; it is obtained using:

$$u_o = \hat{F}_w + T^d - K_o s_o \quad (17)$$

$\hat{F}_w$  is the estimated force due to wind,  $T^d$  is the desired tension required to be maintained in the tether for force-based coordination between the drone and the ground rover and  $K_o > 0$  is the feedback gain matrix.  $s_o$  is the velocity error of the drone and is obtained as<sup>[40,41]</sup>:

$$s_o = \begin{bmatrix} \dot{r}_o^T & \dot{\eta}_o^T \end{bmatrix}^T - \begin{bmatrix} \dot{r}_{or}^T & (\dot{\eta}_{or})^T \end{bmatrix}^T \quad (18)$$

Here,  $\dot{r}_{or}$  and  $\dot{\eta}_{or}$  are the reference linear and angular velocities of the drone. Similarly, we can write a simple general form of dynamical equations of the ground robot as,

$$F_i + T = M_i(p_i)\ddot{p}_i \quad (19)$$

where,  $p_i = \begin{bmatrix} r_i^T & \eta_i^T \end{bmatrix}^T$  is the position ( $r_i$ ) and orientation ( $\eta_i$ ) vector of the ground robot in the world fame  $W$ .  $M_i$  is the symmetric positive definite inertia mass matrix of the ground robot. Since this paper does not focus on developing a lower-level controller for the ground robot, it is assumed that  $F_i^d = F_i$ ; i.e., its actual actuating force matches the desired actuating force of the ground robot. In other words, the ground robot actuators and controller perform perfectly in producing the desired force. The velocity error of the ground robot is  $s_i = \begin{bmatrix} \dot{r}_i^T & \dot{\eta}_i^T \end{bmatrix}^T - \begin{bmatrix} \dot{r}_{ir}^T & (\dot{\eta}_{ir})^T \end{bmatrix}^T$ . Where  $\dot{r}_{ir}$  and  $\dot{\eta}_{ir}$  are the reference linear and angular velocities of the drone. We use the control law for  $\dot{p}_{ir} = \begin{bmatrix} \dot{r}_{ir}^T & \dot{\eta}_{ir}^T \end{bmatrix}^T$  as,

$$\dot{p}_{ir} = \rho(p_i^d - p_i) + \dot{p}_i^d \quad (20)$$

where  $p_i^d$  is the desired goal position and orientation of the ground robot. Note that we obtain the desired tension in the tether during wind disturbance as:

$$T^d = mk_o(\ddot{r}_{ir} - \ddot{r}_o) \quad (21)$$

where  $k_o$  is a proportional constant.

#### 4. ADAPTIVE CONTROL FOR ESTIMATION OF WIND FORCE

The following theorem is used in this paper to implement the proposed adaptive controller.

**Theorem 1.** Consider a tethered drone system whose dynamics are given by Equations 15 and 19. The given system, using the control law given by 17, is asymptotically stable if the following adaptation law is used:

$$\dot{\hat{F}}_w = -\Gamma s_o \quad (22)$$

where  $\Gamma$  is a symmetric positive definite matrix of tunable parameters.

*Proof.* Using equations 15, 16, 18,

$$M_o \dot{s}_o + C_o s_o = \tilde{F}_w + \Delta T - K_o s_o \quad (23)$$

where  $\tilde{F}_w = \hat{F}_w - F_w$  is the wind parameter error vector, and  $K_o > 0$  is a feedback gain matrix of the drone and  $\Delta T = T^d - T$ . Similarly, for the ground robot, we use Equation 19 to obtain:

$$M_i \dot{s}_i = -\Delta T - K_i s_i \quad (24)$$

Now, we choose the candidate Lyapunov function as follows:

$$V = \frac{1}{2} \left( s_o^T M_o s_o + \tilde{F}_w^T \Gamma^{-1} \tilde{F}_w + s_i^T M_i s_i \right) \quad (25)$$

Then, Equations 22, 23, and 24 are used to compute the time derivative of Equation 25. It should be noted that considering the duality of force and velocity and the fact that the force applied by the ground rover via the tether is equal and opposite to the force exerted on the drone (due to the assumption of the mass-less tether), we consider  $s_i = s_o$ . Refer to work of<sup>[40]</sup> for further details. Thus, we have:

$$\begin{aligned} \dot{V} &= s_o^T (\tilde{F}_w + \Delta T - K_o s_o) + s_i^T (-K_i s_i - \Delta T) + \tilde{F}_w^T \Gamma^{-1} \dot{\tilde{F}}_w \\ &= -s_o^T K_o s_o - s_i^T K_i s_i \leq 0 \end{aligned} \quad (26)$$

$\dot{V}$  is negative semi-definite. Thus,  $s_o$ ,  $\tilde{F}_w$  and  $s_i$  are bounded. Since  $\tilde{F}_w$  is bounded,  $\hat{F}_w$  is also bounded as  $F_w$  is considered constant in this paper. From Equation 18,  $p_{or}$ ,  $\dot{p}_{or}$ ,  $\ddot{p}_{or}$ ,  $p_o$ ,  $\dot{p}_o$  and  $\ddot{p}_o$  are bounded considering the operating regime under the small angle approximation. Similarly, from definition of  $s_i$ , we have  $p_{ir}$ ,  $\dot{p}_{ir}$ ,  $\ddot{p}_{ir}$ ,  $p_i$ ,  $\dot{p}_i$  and  $\ddot{p}_i$  to be bounded. Thus, from Equation 21,  $T^d$  is bounded. Hence, referring to Equation 17,  $u_o$  is bounded, and thus, from Equation 15,  $T$  is bounded, which makes  $\Delta T$  bounded. Taking the second derivative of  $V$ , we get,

$$\ddot{V} = -2(s_o^T K_o s_o + s_i^T K_i s_i) \quad (27)$$

From Equations 23 and 24,  $\dot{s}_i$  and  $\dot{s}_o$  are bounded. Thus,  $\ddot{V}$  is bounded according to Barbalat's lemma. Therefore,  $\dot{V} \rightarrow 0$  as  $t \rightarrow \infty$  making  $s_i \rightarrow 0$ ,  $s_o \rightarrow 0$ ,  $\dot{p}_o \rightarrow \dot{p}_{or}$ ,  $\dot{p}_i \rightarrow \dot{p}_{ir}$ ,  $\ddot{p}_{or} \rightarrow 0$  as  $t \rightarrow \infty$ . Thus,  $p_i \rightarrow p_i^d$  and  $T \rightarrow T^d$  as  $t \rightarrow \infty$ . It should be noted that this analysis does not guarantee parameter convergence to true values as condition for persistent excitation has not been implemented.

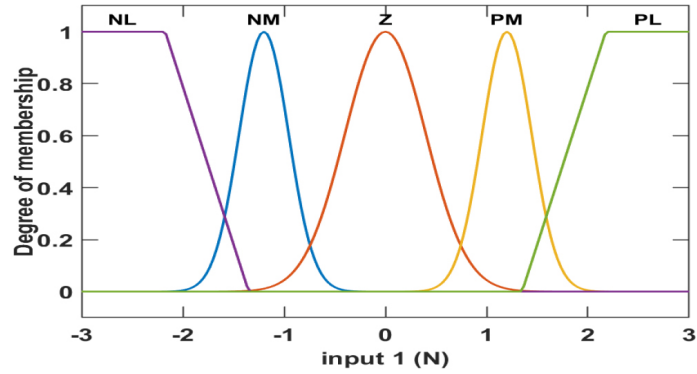
## 5. APPROACH

### 5.1. Fuzzy logic force feedback controller

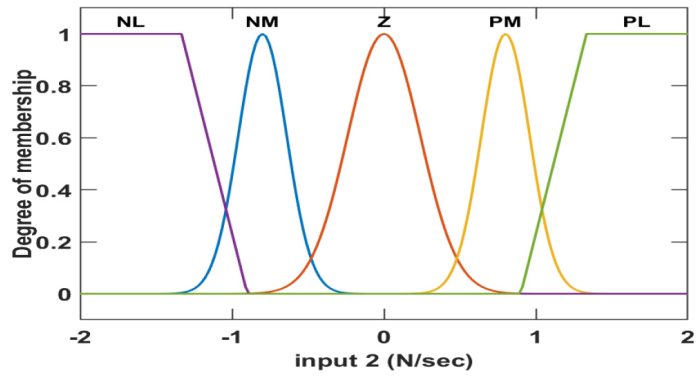
Based on our earlier work<sup>[11,42]</sup>, we propose a fuzzy logic-based force feedback controller to control the pitch and yaw angles of the drone based on the tether forces and their rates acting on the drone due to the motion of the ground rover. Initially, before the ground robot starts moving, the drone goes into its equilibrium position with orientation as  $\eta_o = \begin{bmatrix} 0 & \theta_o^{eq} & 0 \end{bmatrix}^T$ . This orientation maintains an equilibrium tension  $T^{eq} = \begin{bmatrix} T_x^{eq} & 0 & T_z^{eq} \end{bmatrix}^T$  in the tether and also makes the tether inclined to the ground at an angle  $\alpha^{eq}$  (see Equations 4 to 8). After reaching this equilibrium position, the ground robot starts navigating towards its goal location. The next step consists of computing the desired pitch  $\theta_o^f$  and yaw  $\psi_o^f$  angles of the drone based on contact forces and their rates thus making the drone coordinate with the rover via force feedback. Consequently, when the rover moves along the  $X_w$  direction, the drone pitches accordingly, while when the rover moves along the  $Y_w$  axis, it creates a force on the drone along the  $Y_w$  axis making the drone yaw with an objective of aligning its body pitch direction ( $X_B$ ) with the current direction of motion of the rover. Finally, the net desired pitch  $\theta_o^d$  is calculated and commanded to the attitude controller of the drone.

This section presents the fuzzy-based approach used to find  $\theta_o^f$  and  $\psi_o^f$ . Two fuzzy controllers are implemented for pitching and yawing actions, respectively. For calculating  $\theta_o^f$ , two inputs to the fuzzy logic force feedback controller are considered: i) force  $F_x^m - T_x^{eq}$ , and ii) rate of force change  $\dot{F}_x^m$ . Since the first input of the fuzzy logic controller for pitch axis  $F_x^m - T_x^{eq}$  is proportional to the sensed force along the  $X_w$  axis by the drone, we call this controller a force feedback controller. Five membership functions are considered for both the inputs and the output of this controller. The membership functions are negative large (NL), negative medium (NM), Zero (Z), positive medium (PM), and positive large (PL). Table 1 summarizes the fuzzy rule base. The rule base is built using human intuition which can be understood as follows. Let us consider an example when the input  $F_x^m - T_x^{eq}$  is PL and another input  $\dot{F}_x^m$  is NL. In such a scenario, a PL first input  $F_x^m - T_x^{eq}$  means that high force is acting on the drone due to motion of the rover and the drone is supposed to move faster with a large pitch value. However, the second NL input to the fuzzy controller  $\dot{F}_x^m$  means that the rate of contact force change is large in the opposite manner; thus, the contact force is expected to increase in magnitude in a negative direction, which means that the drone should pitch negatively. The net effect of the two inputs is that the drone should not pitch at all; thus, the desired pitch angle (output)  $\theta_o^f$  should then be Z. Similarly, when  $F_x^m - T_x^{eq}$  is PM and  $\dot{F}_x^m$  is PL,  $\theta_o^f$  is chosen as PL. The drone thus compromises between the applied force and its rate of change. This approach is termed the minimization principle of contact forces, where, in order for the drone to move cooperatively with the ground rover, the drone must minimize the contact forces acting at its end due to motion of the ground rover<sup>[11]</sup>. The fuzzy logic controller provides interpretability by providing a linguistic representation where output (control action) is related to inputs (force and rate of change of force) via an intuitive rule base. Figures 2 and 3 show the membership functions and control surface of the fuzzy logic-based force feedback controller along pitch direction while Table 1 shows the fuzzy rules used in simulations. It should be noted that the membership functions were chosen to be Gaussian to maintain continuity and enable gradual transition from one membership function to another during control; this avoids peaks/spikes in output signal.

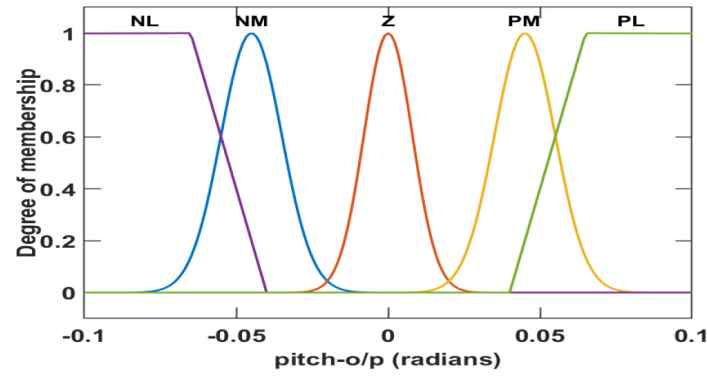
The yaw motion controller is similar to the pitch axis controller except that the first input is  $F_y^m$ . The yaw axis figures are not indicated here for brevity purposes. The outputs of fuzzy-based force feedback controllers along pitch and yaw axes are used to obtain the net desired attitude commands using Equations 11 and 12. The net desired attitude commands are used by the attitude controller of the drone to control the rotor speeds using Proportional-Derivative controllers (see<sup>[39,43]</sup> for more details). Figure 4 illustrates the control architecture of the system with fuzzy logic force feedback controller for a tethered drone, and more details are provided.



(a) Membership functions of input 1 ( $F_x^m - T_x^{eq}$ ).



(b) Membership functions of input 2 ( $\dot{F}_x^m$ ).



(c) Output membership functions of desired pitch angle  $\theta_o^f$ .

**Figure 2.** Simulations: Membership functions for fuzzy logic force feedback controller in pitch direction.

### 5.2. Proportional controller for wind disturbance

We now present another controller for the tethered drone for wind disturbance analysis. Once the input  $u_o$  is computed, the desired pitch  $\theta_o^f$  and yaw  $\psi_o^f$  angles based on forces are then calculated using a proportional controller as

$$\theta_o^f = k_{t,\theta}^p (u_{o,x} + F_x^m) \tag{28}$$

and

$$\psi_o^f = k_{t,\psi}^p (u_{o,y} + F_y^m) \tag{29}$$

where  $k_{t,\theta}^p$  and  $k_{t,\psi}^p$  are the proportional gains. Please note that the symbols used in all sections have been kept the same to maintain consistency. The wind analysis control part of this paper is different from the fuzzy logic

**Table 1. Simulations: Fuzzy logic rules of force feedback controller for the pitch direction**

		input 1				
		NL	NM	Z	PM	PL
input 2	NL	NM	NM	NM	Z	Z
	NM	NL	NM	Z	Z	Z
	Z	NM	NM	Z	PM	PM
	PM	NM	Z	PM	PM	PM
	PL	Z	Z	PM	PL	PL

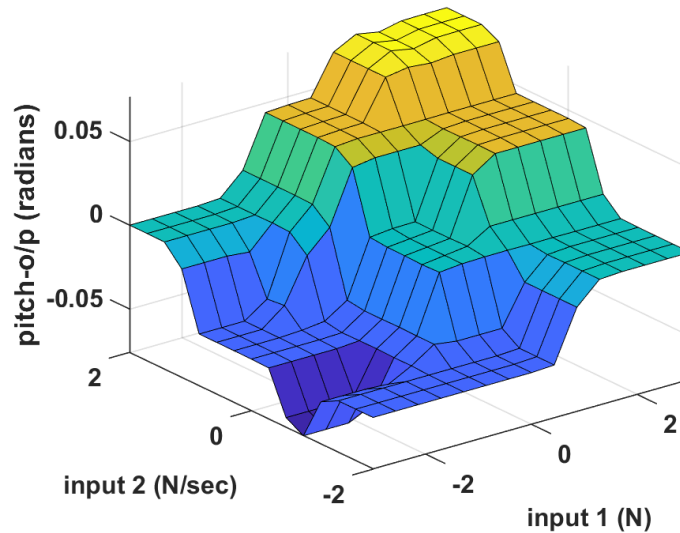


**Figure 3.** Simulations: Control surface of the fuzzy logic force feedback controller along pitch direction.

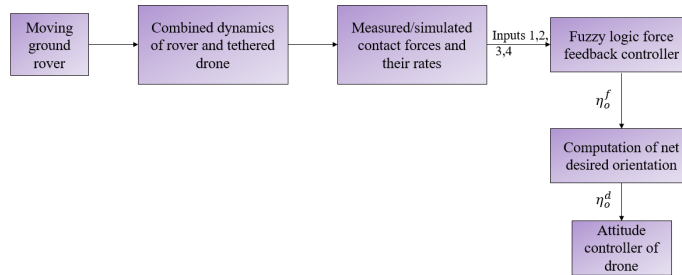


**Figure 4.** Fuzzy logic force feedback controller: Control architecture of the entire system.

control part presenting the active control of the tethered drone without presence of wind. The wind analysis section is just proposed as an additional preliminary work, and in the future, we plan to apply a fuzzy scheme for it.

### 5.3. Attitude controller of drone

Based on the computed  $\phi_o^d$ ,  $\theta_o^d$  and  $\psi_o^d$ , we compute the deviations from  $\omega_o^h$  for different rotors used to navigate the drone along different directions. These deviations  $\Delta\omega_o^\phi$ ,  $\Delta\omega_o^\theta$  and  $\Delta\omega_o^\psi$  are computed by implementing

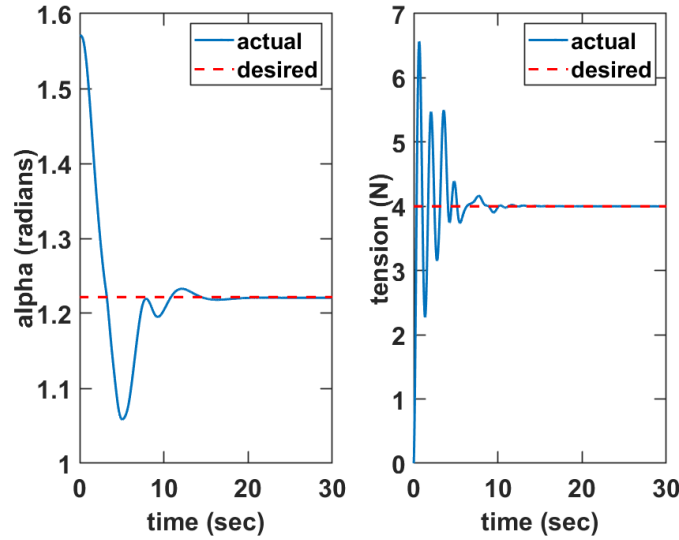


**Figure 5.** Simulations: Graph showing the angle ( $\alpha$ ) the tether makes with the ground and the tether tension ( $T$ ).

proportional-derivative (PD) controllers as follows,

$$\Delta\omega_o^\phi = k_{\eta,\phi}^p(\phi_o^d - \phi) + k_{\dot{\eta},\phi}^d(\dot{\phi}_o^d - \dot{\phi}) \quad (30)$$

$$\Delta\omega_o^\theta = k_{\eta,\theta}^p(\theta_o^d - \theta) + k_{\dot{\eta},\theta}^d(\dot{\theta}_o^d - \dot{\theta}) \quad (31)$$

$$\Delta\omega_o^\psi = k_{\eta,\psi}^p(\psi_o^d - \psi) + k_{\dot{\eta},\psi}^d(\dot{\psi}_o^d - \dot{\psi}) \quad (32)$$

where,  $k_{\eta,\phi}^p$ ,  $k_{\eta,\theta}^p$  and  $k_{\eta,\psi}^p$  are the proportional gains and  $k_{\dot{\eta},\phi}^d$ ,  $k_{\dot{\eta},\theta}^d$  and  $k_{\dot{\eta},\psi}^d$  are the derivative gains of the PD controller. The desired individual rotor speeds of the drone are then computed based on  $\Delta\omega_o^\phi$ ,  $\Delta\omega_o^\theta$  and  $\Delta\omega_o^\psi$  using a control allocation matrix<sup>[39]</sup>.

## 6. RESULTS

This section presents results for simulations and experiments of the proposed controller. The simulation results consist of implementation of a fuzzy logic force feedback controller and validation of a proportional controller for wind disturbance analysis. MATLAB is used to simulate the system. Experimental work comprises validation of the proposed fuzzy logic force feedback controller using a Crazyflie drone attached to a TurtleBot.

### 6.1. Simulations

#### *Fuzzy logic force feedback controller*

**Simulation setup and parameters** - A drone of mass  $m = 1\text{ kg}$  is tethered to a ground rover of mass  $3\text{ kg}$ . The desired tension in the tether is chosen as  $T^d = T^{eq} = 4\text{ N}$ , while the desired angle of the tether with the ground is  $\alpha^d = \alpha^{eq} = 70^\circ = 1.22\text{ rad}$ . The desired pitch angle at equilibrium position is  $\theta_o^{eq} = 5.75^\circ = 0.1\text{ rad}$ . The ground robot is required to reach the goal location of  $(-5\text{ m}, 5\text{ m})$ . The tether is chosen to have stiffness  $K = 20\text{ N/m}$ , damping  $C = 1\text{ Nsec/m}$ , and length  $l = 5\text{ m}$ . Other parameters used in simulation are:  $L = 0.12\text{ m}$ ,  $k_\eta^p = \begin{bmatrix} 100 & 100 & 100 \end{bmatrix}^T$ ,  $k_{\dot{\eta}}^d = \begin{bmatrix} 20 & 20 & 20 \end{bmatrix}^T$ ,  $k_g^p = \begin{bmatrix} 0.4 & 0.4 \end{bmatrix}^T$ ,  $k_g^d = \begin{bmatrix} 1 & 1 \end{bmatrix}^T$ . The fuzzy membership functions were chosen to be Gaussian to maintain continuity and enable gradual transition from one membership function to another during control; this avoids peaks/spikes in the output signal.

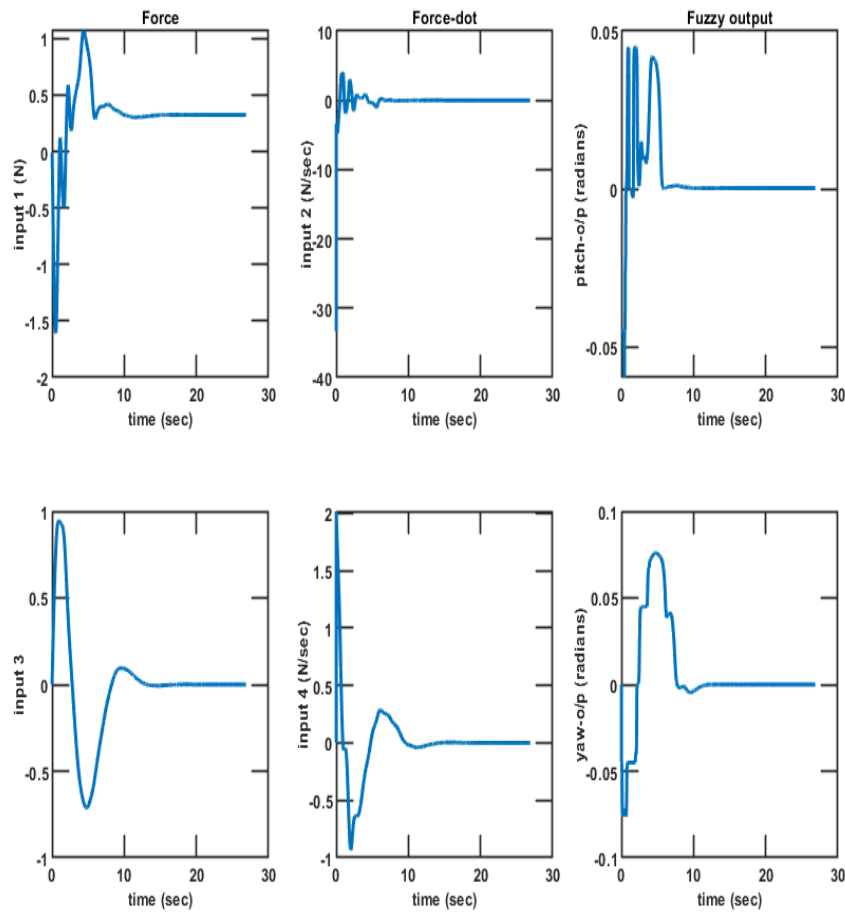


**Figure 6.** Simulations: Graph showing the inputs and outputs of fuzzy logic force feedback controllers for pitch (top row) and yaw angles (bottom row). Input 1 is  $F_x^m - T_x^{eq}$ , Input 2 is  $F_x^m$ , Input 3 is  $F_y^m$  and Input 4 is  $F_y^m$ .

**Results** - Figure 5 shows the tension change in the tether and the angle  $\alpha$  made by the tether with the ground. It can be seen that the drone tries to maintain the desired values of tension and angle with the ground. Figure 6 presents the inputs and outputs generated by the fuzzy controller for both pitch and yaw axes. The top row demonstrates the inputs and output for the pitch controller, and the bottom row indicates the inputs and output for the yaw controller. Figure 7 exhibits the position of the ground robot and the drone during the simulation period. It can be seen that both the ground rover and the drone stably reach their specified goal locations starting from their initial points. Please note the slight offset between desired and actual position values along the  $Z_W$  direction. This is expected since we do not implement any controller along the vertical  $Z_W$  axis of the drone. The rightmost column of Figure 7 shows the net desired pitch and yaw angles ( $\theta_o^d$  and  $\psi_o^d$ ) commanded to the attitude controller of the drone. It can be observed that the attitude controller of the drone stably tracks the desired values.

*Proportional controller for wind disturbance analysis*

**Simulation setup and parameters** - For simulation study of the system under wind disturbance, we chose the following system parameters. The mass of a drone is taken as  $m = 1\text{ kg}$ , while the ground rover has a mass of  $3\text{ kg}$ . The desired tension in the tether is chosen as  $T^d = T^{eq} = 4\text{ N}$ , while the desired angle of the tether with the ground is  $\alpha^d = \alpha^{eq} = 70^\circ = 1.22\text{ rad}$ . The desired pitch angle at equilibrium position is  $\theta_o^{eq} = 5.75^\circ = 0.1\text{ rad}$ . The ground robot is required to reach the goal location of  $(-5\text{ m}, 3\text{ m})$ . The tether is chosen to have stiffness

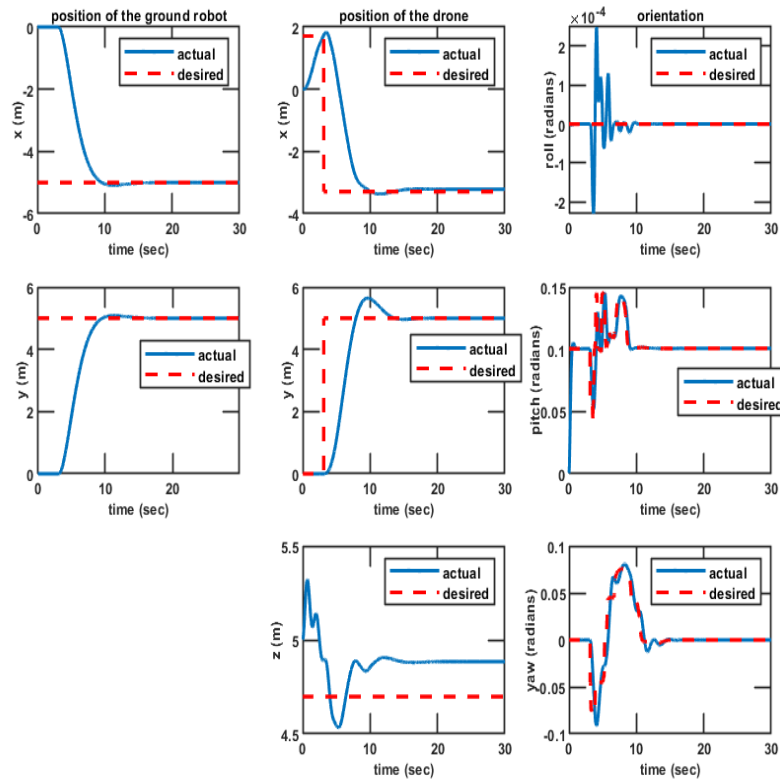


**Figure 7.** Simulations: Graph showing the desired and actual position of the ground rover and the drone. The left column shows the ground robot position (actual and desired). The middle column shows the drone position (actual and desired). The rightmost column shows the net desired and actual roll, pitch, and yaw angles.

$K = 20N/m$ , damping  $C = 1Nsec/m$ , and length  $l = 5m$ . A constant wind force of  $6N$  along the  $X_W$  direction and  $1N$  along the  $Y_W$  direction is applied at  $t=4$  sec and persists till the end of the simulation. Other parameters are:  $L = 0.12m$ ,  $k_{\eta}^p = [100 \ 100 \ 100]^T$ ,  $k_{\eta}^d = [20 \ 20 \ 20]^T$ ,  $k_{t,\theta}^p = 0.01$ ,  $k_{t,\psi}^p = 0.01$ ,  $k_g^p = [1 \ 0.1]^T$ ,  $k_g^d = [1 \ 1]^T$ ,  $K_o = diag(0.01 \ 0.01 \ 0)$ ,  $\Gamma = diag(0.22 \ 1 \ 0)$ .

**Results** - The results for this subsection are shown in Figures 8 and 9. It can be seen from Figure 8 that both the ground robot and the drone reach their respective goal locations in presence of wind disturbance. The vertical motion along the  $Z_W$  axis is not controlled; hence, slight offset is seen between the desired and actual altitude values. The attitude controller of the drone also tracks its desired orientation well. Figure 9 shows that the adaptive controller computes the estimate of the unknown wind disturbance effectively. Adaptive estimate of wind force is then used to control the tethered drone, as presented in Section 5. Figure 10 further presents the stable flight of the tethered drone in windy environments. The green dashed line indicates the trajectory of the drone, while the red denotes the path of the ground robot. The blue and the red arrows depict the lateral wind forces acting on the drone. It should be noted that the wind disturbance is assumed to be along the lateral  $X_W Y_W$  plane.

### 6.2. Experiments to validate the fuzzy logic controller

For experimental validation of the fuzzy logic controller, TurtleBot 3 Burger<sup>[44]</sup> and Crazyflie 2.1<sup>[45]</sup> were used as the ground robot and quadrotor drone, respectively. The drone was tethered to the turtle bot by a tether. Figure 11 shows the system of the Crazyflie tethered to the TurtleBot. We use Raspberry Pi (Rpi) as

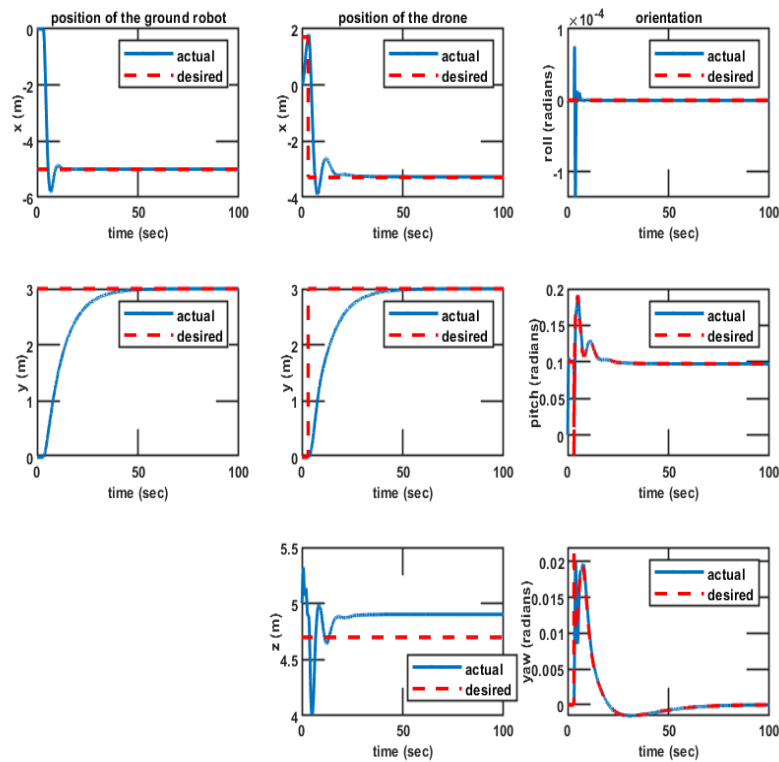


**Figure 8.** Simulations: Graph showing the position of the drone and the ground robot under wind disturbances. The left column shows the ground robot position (actual and desired). The middle column shows the drone position (actual and desired). The rightmost column shows the net desired and actual roll, pitch, and yaw angles.

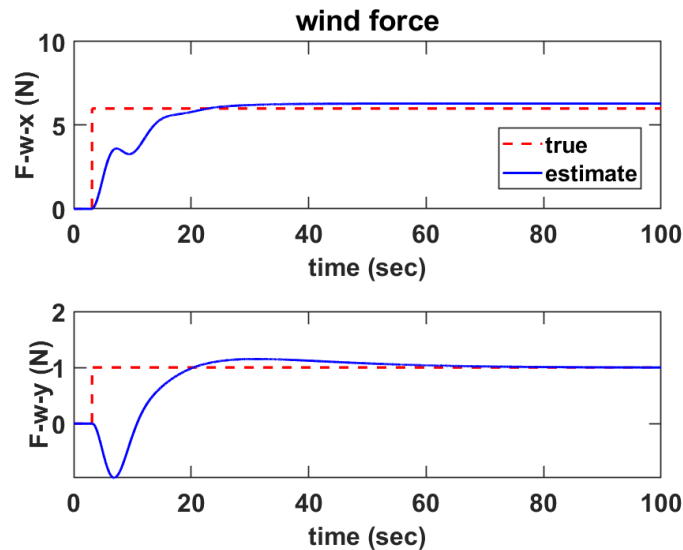


**Figure 9.** Simulations: Graph showing the estimate of the constant unknown wind force/disturbance on the drone using the proposed adaptive control strategy.

an onboard computer on the TurtleBot which sends commands to the Crazyflie via a Radio attached to the Rpi. Two inexpensive noisy load cells (attached to the ground rover) are employed to measure forces in the

$X_W Y_W$  plane. A/D amplifying converters are also applied along with the load cells. Notably, since tension in tether is equal and opposite at the two ends, i.e., the drone and the ground rover, this allows us to attach the force sensor to the ground rover instead of the drone. It may be noted that this requires properly taking care of the directions of the forces when controlling the drone based on them. Further, the onboard computer, Rpi, gathers load cell data, applies a Kalman filter for the data, and then implements the proposed fuzzy logic force feedback controller. The fuzzy controller then generates the desired pitch and yaw angles and then uses them to calculate the net desired pitch and yaw angles. The net desired pitch and yaw angles are then commanded to the attitude controller of the Crazyflie. It should be noted that the Crazyflie is made to fly at constant thrust. The parameters used in experiments for the Crazyflie platform are  $thrust = 40000$  and  $\theta_o^{eq} = 4^\circ = 0.07rad$ .

Figures 12 and 13 demonstrate the membership functions and control surface of the fuzzy logic force feedback controller used in experiments. The fuzzy rules are similar to those used for simulations and, thus, are not indicated in this subsection. Two cases are evaluated in the experiments: i) Case 1: Straight line motion and ii) Case 2: Circular trajectory tracking. The results along the  $X_W$  or pitch axis for Case 1 are shown in Figure 14. It can be seen that the fuzzy logic controller effectively generates the pitch output based on forces and their rates ( $F_x^m - T_x^{eq}$  and  $\dot{F}_x^m$ ). Moreover, the attitude tracking controller of the Crazyflie tracks the desired pitch angle well. The black dashed line marked on the bottom plot of Figure 14 shows the equilibrium pitch angle  $\theta_o^{eq}$  for Case 1 about which the net desired pitch angle  $\theta_o^d$  varies. Figure 15 presents the results for yaw control for Case 1 based on forces and their rates ( $F_y^m$  and  $\dot{F}_y^m$ ). The yaw rate controller of the Crazyflie shows successful tracking of the desired yaw rate. It should be noted that, given hardware constraints, we decided to command the yaw rate to the Crazyflie instead of the desired yaw angle based on force feedback. It can be seen from these results that the drone can be actively manipulated by the ground rover as if the ground robot is flying the drone akin to a kite. Figures 16 and 17 exhibit similar results for Case 2 when the ground robot is made to move along a circular path performing the trajectory tracking. These results show that irrespective of whether the ground robot moves in a straight line or tracks a trajectory, the drone can coordinate with it via forces and their rates.

The results in this section validate the performance of the proposed approach for an actively manipulated tethered drone.

## 7. CONCLUSIONS

This paper focuses on developing and demonstrating a control approach for actively manipulating drones tethered to a ground robot. We presented a fuzzy logic-based force feedback controller for such a tethered drone system where the drone coordinated with the moving ground rover using the measured contact forces due to the tether. Fuzzy logic allows effective force coordination between the ground rover and the drone, incorporation of human knowledge in controller design, and use of noisy, inexpensive force sensors. Additionally, fuzzy logic provides explainability to the control engineer regarding the decisions the controller takes. Both simulation and experimental results are provided, which validate the performance of the proposed controller. This paper additionally implements a proportional force-based controller to control a tethered drone during wind disturbances. The proposed technique uses an adaptation law to estimate unknown winds and uses that information to control the drone. The simulation results of wind disturbance analysis are presented to support the proposed approach. Future work consists of implementing a fuzzy logic controller for the system during wind disturbances and developing adaptive strategies for such a system during time-varying winds. Current novel state-of-the-art on channel estimation, link and parameters for drone and ground rover communication with posture variation, fuselage scattering effect and utilization of machine learning for 3D channel monitoring is worth noting and can also be incorporated in this research as a part of future work [46–48].

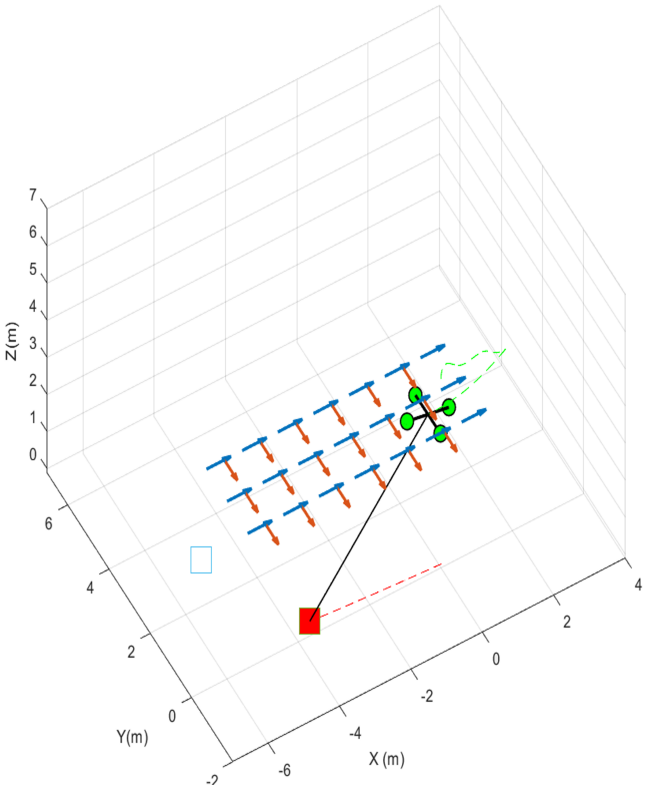


Figure 10. Simulations: Tethered drone flying in a simulated environment with wind disturbance.

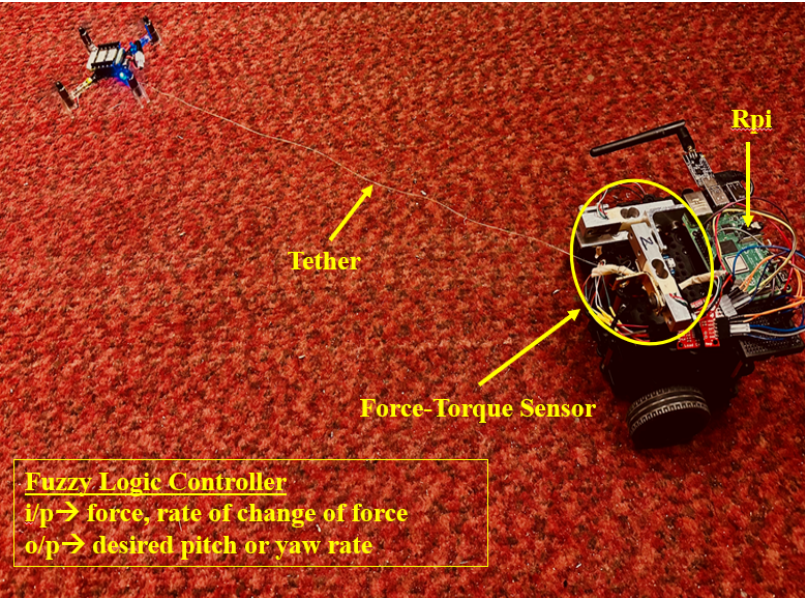
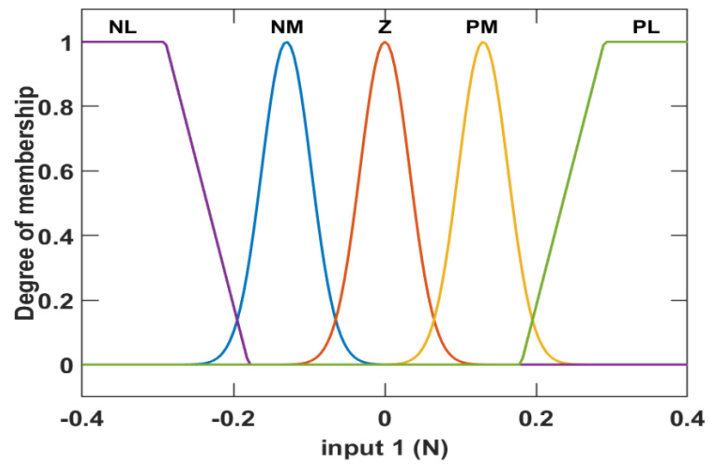
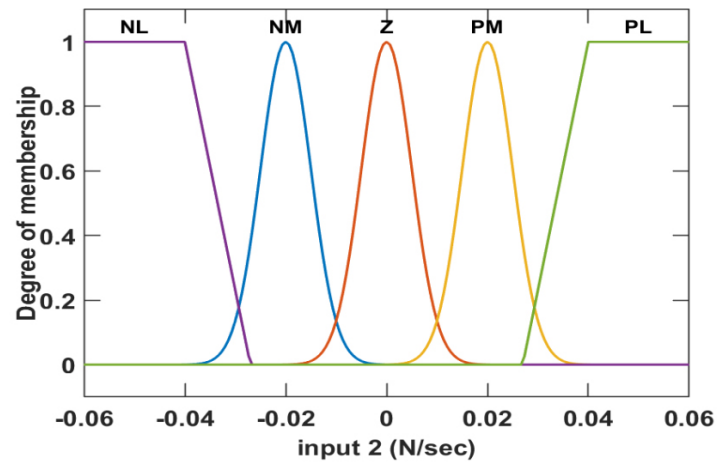


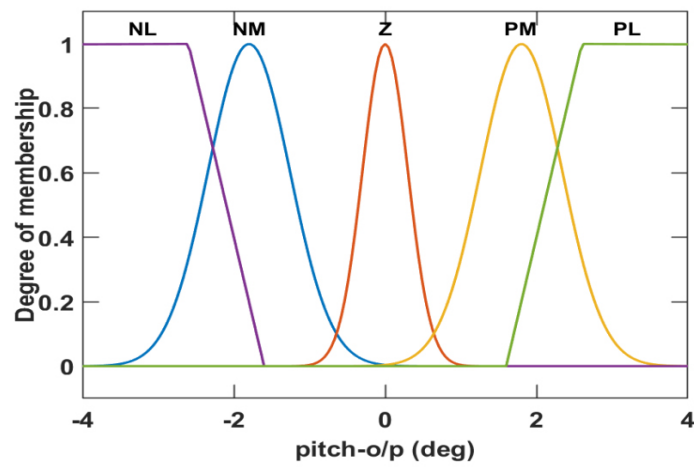
Figure 11. Experiments: Schematic diagram of the system used in experiments.



(a) Membership functions of input 1 ( $F_x^m - T_x^{eq}$ ).



(b) Membership functions of input 2 ( $\dot{F}_x^m$ ).



(c) Output membership functions of desired pitch angle  $\theta_o^f$ .

Figure 12. Experiments: Membership functions for fuzzy logic force feedback controller in pitch direction.

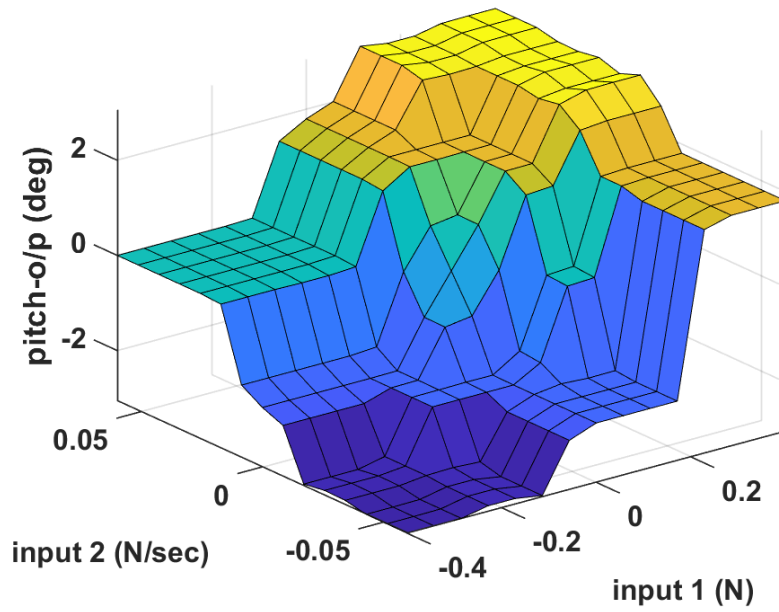


Figure 13. Experiments: Control surface of the fuzzy logic force feedback controller along pitch direction.

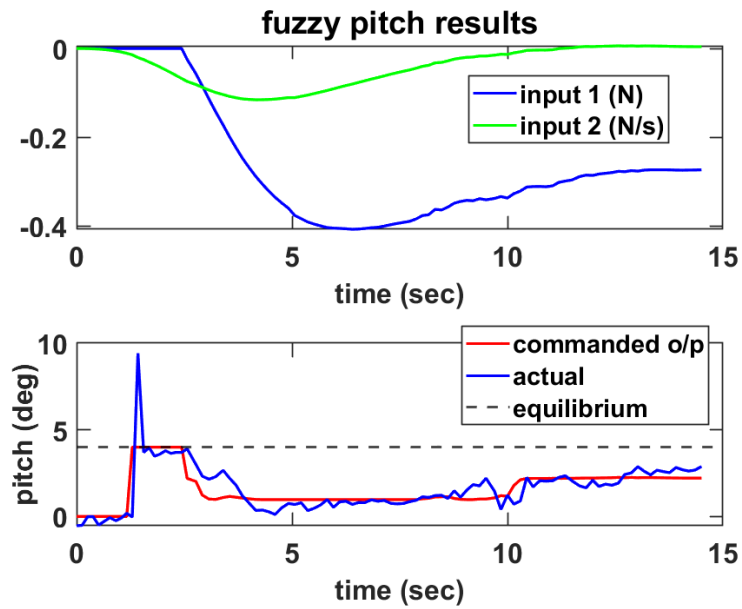
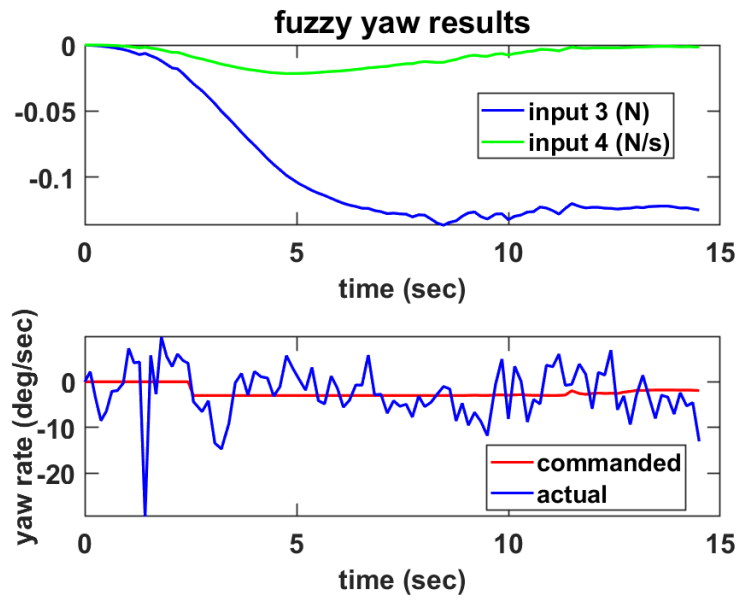
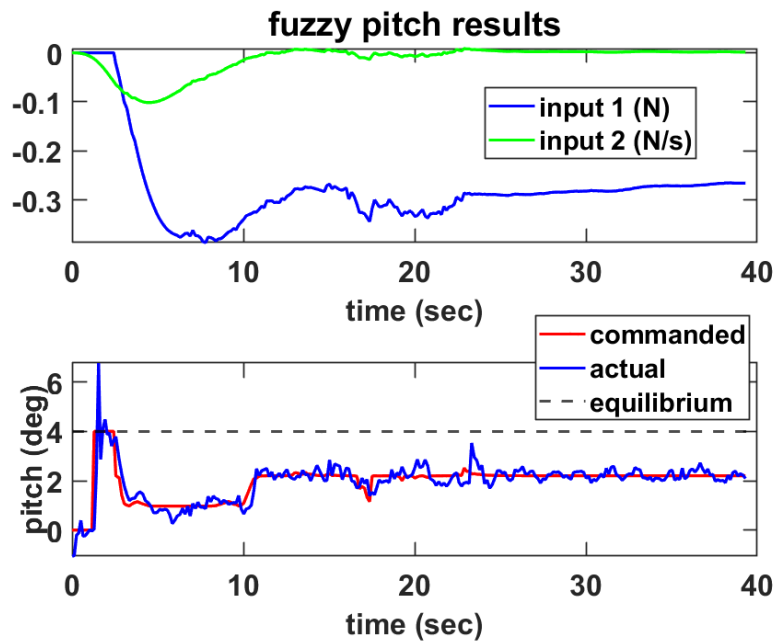


Figure 14. Experiments (Case 1: Straight line motion): Graph showing the inputs - forces and their rates ( $F_x^m - T_x^{c,q}$  and  $\dot{F}_x^m$ ) -acting on the drone along the pitch direction. The bottom plot shows the desired net pitch angle  $\theta_o^d$  and the actual pitch angle  $\theta_o$ . The black dashed line on the bottom plot shows marks the desired equilibrium pitch angle  $\theta_o^{e,q}$ .



**Figure 15.** Experiments (Case 1: Straight line motion): Graph showing the inputs - forces and their rates ( $F_y^m$  and  $\dot{F}_y^m$ ) -acting on the drone for yaw control. The bottom plot shows the desired yaw rate  $\dot{\psi}_o^d$  and the actual yaw rate  $\dot{\psi}_o$ .



**Figure 16.** Experiments (Case 2: Circular trajectory tracking): Graph showing the inputs - forces and their rates ( $F_x^m - T_x^{c,q}$  and  $\dot{F}_x^m$ ) -acting on the drone along the pitch direction. The bottom plot shows the desired net pitch angle  $\theta_o^d$  and the actual pitch angle  $\theta_o$ . The black dashed line on the bottom plot shows marks the desired equilibrium pitch angle  $\theta_o^{c,q}$ .

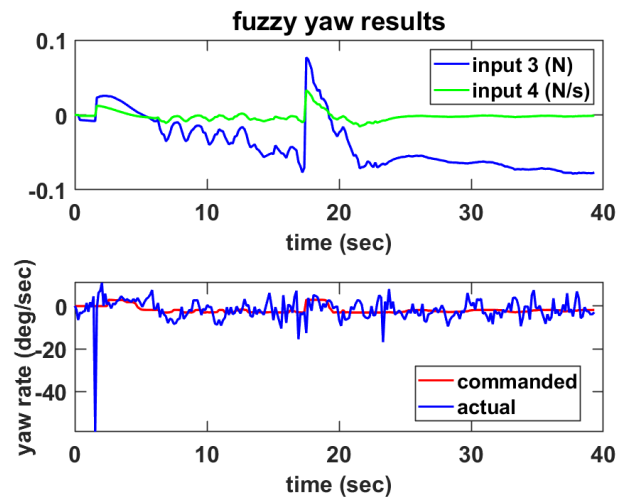


**Figure 17.** Experiments (Case 2: Circular trajectory tracking): Graph showing the inputs - forces and their rates ( $F_y^m$  and  $\dot{F}_y^m$ ) - acting on the drone for yaw control. The bottom plot shows the desired yaw rate  $\psi_o^d$  and the actual yaw rate  $\psi_o$ .

## 8. PATENTS

This work is based on our recent patent<sup>[21]</sup>.

## DECLARATIONS

### Acknowledgments

We would like to acknowledge the University of Cincinnati's Space Research Institute for Discovery and Exploration (SRIDE) for supporting this research in the form of SRIDE Fellowship to the first author of this paper for the years 2022-23.

### Authors' contributions

Contributed to the proposed methodology, simulation and experimental validation, and draft writing: Barawkar S

Provided regular feedback on all aspects of research, and assisted in writing the manuscript (The second author is the faculty advisor who investigated and supervised the first author): Kumar M

### Availability of data and materials

Not applicable.

### Financial support and sponsorship

The University of Cincinnati's Space Research Institute for Discovery and Exploration (SRIDE) funding support was utilized for this research in the form of SRIDE Fellowship to the first author of this paper for the years 2022-23.

### Conflicts of interest

All authors declared that there are no conflicts of interest.

### Ethical approval and consent to participate

Not applicable.

### Consent for publication

Not applicable.

## Copyright

© The Author(s) 2024.

## REFERENCES

1. Yoo S, Kim S, Kim S, Kang BB. AI-HydRa: advanced hybrid approach using random forest and deep learning for malware classification. *Inf Sci* 2021;546:420–35. DOI
2. Park JH, Farkhodov K, Lee SH, Kwon KR. Deep reinforcement learning-based DQN agent algorithm for visual object tracking in a virtual environmental simulation. *Appl Sci* 2022;12:3220. DOI
3. Fragkos G, Tsiropoulou EE, Papavassiliou S. Disaster management and information transmission decision-making in public safety systems. In: 2019 IEEE Global Communications Conference (GLOBECOM). IEEE; 2019. pp. 1–6. DOI
4. Salehinejad H, Sankar S, Barfett J, Colak E, Valae S. Recent advances in recurrent neural networks. *arXiv preprint arXiv:180101078* 2017. DOI
5. Osco LP, Junior JM, Ramos APM, et al. A review on deep learning in UAV remote sensing. *Int J Appl Earth Obs Geoinf* 2021;102:102456. DOI
6. Gunning D, Stefik M, Choi J, et al. XAI—Explainable artificial intelligence. *Sci Robot* 2019;4:eaay7120. DOI
7. Keneni BM, Kaur D, Al Bataineh A, et al. Evolving rule-based explainable artificial intelligence for unmanned aerial vehicles. *IEEE Access* 2019;7:17001–16. DOI
8. Došilović FK, Brčić M, Hlupić N. Explainable artificial intelligence: A survey. In: 2018 41st International convention on information and communication technology, electronics and microelectronics (MIPRO). IEEE; 2018. pp. 0210–15. DOI
9. Samek W, Müller KR. Towards explainable artificial intelligence. Explainable AI: Interpreting, Explaining and Visualizing Deep Learning. Cham: Springer International Publishing; 2019. pp. 5–22. DOI
10. Lima BN, Balducci P, Passos RP, et al. Artificial intelligence based on fuzzy logic for the analysis of human movement in healthy people: a systematic review. *Artif Intell Rev* 2021;54:1507–23. DOI
11. Barawkar S, Kumar M. Force-torque (FT) based multi-drone cooperative transport using fuzzy logic and low-cost and imprecise FT sensor. *Proc Inst Mech Eng G J Aerosp Eng* 2023:09544100231153686. DOI
12. De Reus N. Assessment of benefits and drawbacks of using fuzzy logic, especially in fire control systems. FYSISCH EN ELEKTRONISCH LAB TNO THE HAGUE (NETHERLANDS); 1994.
13. Albertos P, Sala A. Fuzzy logic controllers. Advantages and drawbacks. In: VIII international congress of automatic control. vol. 3; 1998. pp. 833–44.
14. Dewi T, Nurmaini S, Risma P, Oktarina Y, Roriz M. Inverse kinematic analysis of 4 DOF pick and place arm robot manipulator using fuzzy logic controller. *Int J Electr Comput Eng* 2020;10:1376. DOI
15. Štefek A, Pham VT, Krivanek V, Pham KL. Optimization of fuzzy logic controller used for a differential drive wheeled mobile robot. *Appl Sci* 2021;11:6023. DOI
16. Mishra DK, Thomas A, Kuruvilla J, et al. Design of mobile robot navigation controller using neuro-fuzzy logic system. *Comput Electr Eng* 2022;101:108044. DOI
17. Lim S, Yu H, Lee H. Optimal tethered-UAV deployment in A2G communication networks: Multi-agent Q-learning approach. *IEEE Internet Things J* 2022;9:18539–49. DOI
18. Elistair;. Available from: <https://elistair.com/>. [Last accessed on 18 Mar 2024]
19. Fotokite;. Available from: <https://fotokite.com/>. [Last accessed on 18 Mar 2024]
20. Hoverfly; 2021. Available from: <https://hoverflytech.com/>. [Last accessed on 18 Mar 2024]
21. Barawkar S, Kumar M, Cohen K. Tether controlled drone. Google Patents; 2022. US Patent App. 17/385,026.
22. Barawkar S, Radmanesh M, Kumar M, Cohen K. Fuzzy logic based variable damping admittance control for multi-UAV collaborative transportation. In: 2018 Annual American Control Conference (ACC). IEEE; 2018. pp. 2084–89. DOI
23. Barawkar S, Radmanesh M, Kumar M, Cohen K. Admittance based force control for collaborative transportation of a common payload using two uavs. In: ASME 2017 Dynamic Systems and Control Conference. American Society of Mechanical Engineers Digital Collection; 2017. DOI
24. Augugliaro F, D’Andrea R. Admittance control for physical human-quadcopter interaction. In: 2013 European Control Conference (ECC). IEEE; 2013. pp. 1805–10. DOI
25. Breese B, Scott D, Barawkar S, Kumar M. Fuzzy logic controller for force feedback control of quadcopter via tether. In: Dynamic Systems and Control Conference. vol. 84287. American Society of Mechanical Engineers; 2020. p. V002T36A008. DOI
26. Ghamry KA, Dong Y, Kamel MA, Zhang Y. Real-time autonomous take-off, tracking and landing of UAV on a moving UGV platform. In: 2016 24th Mediterranean conference on control and automation (MED). IEEE; 2016. pp. 1236–41. DOI
27. Guérin F, Guinand F, Brethé JF, et al. UAV-UGV cooperation for objects transportation in an industrial area. In: 2015 IEEE International Conference on Industrial Technology (ICIT). IEEE; 2015. pp. 547–52. DOI
28. Fagiano L. Systems of tethered multicopters: modeling and control design. *IFAC-PapersOnLine* 2017;50:4610–15. DOI
29. Martinez Rocamora Jr B, Lima RR, Samarakoon K, et al. Oxpecker: A tethered uav for inspection of stone-mine pillars. *Drones* 2023;7:73. DOI
30. Lee T. Geometric controls for a tethered quadrotor UAV. In: 2015 54th IEEE conference on decision and control (CDC). IEEE; 2015. pp.

- 2749–54. DOI
31. Kourani A, Daher N. Marine locomotion: A tethered UAV-buoy system with surge velocity control. *Rob Auton Syst* 2021;145:103858. DOI
  32. Glick T, Arogeti S. Control of tethered drones with state and input constraints-a unified model approach. In: 2018 International Conference on Unmanned Aircraft Systems (ICUAS). IEEE; 2018. pp. 995–002. DOI
  33. Sandino LA, Bejar M, Kondak K, Ollero A. On the use of tethered configurations for augmenting hovering stability in small-size autonomous helicopters. *J Intell Robot Syst* 2013;70:509–25. DOI
  34. Nicotra MM, Naldi R, Garone E. Nonlinear control of a tethered UAV: The taut cable case. *Automatica* 2017;78:174–84. DOI
  35. Mokhtari A, Benallegue A. Dynamic feedback controller of Euler angles and wind parameters estimation for a quadrotor unmanned aerial vehicle. In: IEEE International Conference on Robotics and Automation, 2004. Proceedings. ICRA'04. 2004. vol. 3. IEEE; 2004. pp. 2359–66. DOI
  36. Ali ZA, Zhangang H. Maneuvering control of hexrotor UAV equipped with a cable-driven gripper. *IEEE Access* 2021;9:65308–18. DOI
  37. Escareño J, Salazar S, Romero H, Lozano R. Trajectory control of a quadrotor subject to 2D wind disturbances: Robust-adaptive approach. *J Intell Robot Syst* 2013;70:51–63. DOI
  38. Kumar R, Agarwal SR, Kumar M. Modeling and Control of a Tethered Tilt-Rotor Quadcopter with Atmospheric Wind Model. *IFAC-PapersOnLine* 2021;54:463–68. DOI
  39. Michael N, Mellinger D, Lindsey Q, Kumar V. Experimental evaluation of multirobot aerial control algorithms. *IEEE Robot Autom Mag* 2010;17:56–65. DOI
  40. Kawasaki H, Ito S, Ramli RB. Adaptive decentralized coordinated control of multiple robot arms. *IFAC Proc Vol* 2003;36:387–92. DOI
  41. Barawkar S, Kumar M. Fuzzy logic force-torque feedback controller for multi-drone cooperative transport with offset cg. *IFAC-PapersOnLine* 2021;54:605–10. DOI
  42. Barawkar S. Collaborative transportation of a common payload using two UAVs based on force feedback control. University of Cincinnati; 2017. Available from: [http://rave.ohiolink.edu/etdc/view?acc\\_num=ucin1505125636211596](http://rave.ohiolink.edu/etdc/view?acc_num=ucin1505125636211596). [Last accessed on 18 Mar 2024]
  43. Barawkar S, Kumar M. Cooperative Transport of a Payload With Offset CG Using Multiple UAVs. In: Dynamic Systems and Control Conference. vol. 59162. American Society of Mechanical Engineers; 2019. p. V003T21A008. DOI
  44. Robotis. TurtleBot 3 Burger; 2023. Available from: <https://www.robotis.us/turtlebot-3-burger-us/>. [Last accessed on 18 Mar 2024]
  45. Bitcraze. Crazyflie 2.1; 2023. Available from: <https://www.bitcraze.io/products/crazyflie-2-1/>. [Last accessed on 18 Mar 2024]
  46. Hua B, Ni H, Zhu Q, et al. Channel modeling for UAV-to-ground communications with posture variation and fuselage scattering effect. *IEEE Trans Commun* 2023;71:3103-16. DOI
  47. Mao K, Zhu Q, Song M, et al. Machine-learning-based 3-D channel modeling for U2V mmWave communications. *IEEE Internet Things J* 2022;9:17592–607. DOI
  48. Mao K, Zhu Q, Qiu Y, et al. A uav-aided real-time channel sounder for highly dynamic non-stationary a2g scenarios. *IEEE Trans Instrum Meas* 2023;72:1-15. DOI